THE BELL SYSTEM TECHNICAL JOURNAL
Vol. 56, No. 10, December 1977
Printed in U.S.A.

WT4 Millimeter Waveguide System:

Spectrum Estimation Techniques for Characterization and Development of WT4 Waveguide—II

By D. J. THOMSON

(Manuscript received April 7, 1977)

In Part I techniques for reliably estimating the power spectral density function for both small and large samples of a stationary stochastic process were described. These techniques have been particularly successful in cases where the range of the spectrum is large. They are resistant to a moderate amount of contaminated or erroneous data. Here these procedures were demonstrated using examples from the development and analysis of the WT4 waveguide medium and compared to conventional techniques.

I. INTRODUCTION

The use of the spectral density function for the characterization of mode conversion effects in millimeter waveguide problems has been in general use since the pioneering paper of Rowe and Warters[2] and has subsequently appeared in several other forms (Morrison and McKenna,[3] Pusey[4]). In this paper the emphasis will not be on mode conversion problems per se but rather on the more fundamental problem of obtaining an accurate estimate of the spectrum for the geometric distortion causing the mode conversion.

In Part I a technique for the estimation of the power spectral density function was described[1] which differs from conventional estimation procedures in several respects. In particular the technique is both *robust*—that is, it is resistant to a moderate amount of erroneous or outlying data—and has the ability to estimate spectra which have very large dynamic ranges. While Part I was primarily theoretical, Part II is devoted primarily to examples of this technique as applied to the analysis

of WT4 waveguide data and comparisons of this method to standard techniques. Because of the complexity of the WT4 system these examples cover a wide range; from the analysis of individual tubes where the sample is very short relative to the resolution required, to the analysis of complete mode filter sections where the amount of data which must be contained in the analysis is almost prohibitive. Some spectra are almost white while some cover ranges of 10 to 16 decades.

Briefly, the method described in Part I begins by forming a *pilot estimate* of the spectrum using a modification of Welch's technique.[5] The pilot estimate is used to form an *autoregressive model* of the process which is used as part of a *robust prewhitening filter.* The final estimate of the spectrum is the *ratio* of the spectrum of the prewhitening residuals to the power transfer function of the autoregressive filter.

While this procedure is clearly motivated by the use of prewhitening techniques it differs from traditional methods in many important aspects:

(*i*) First, extensive use is made of *prolate spheroidal wave functions* as data windows or tapers. These functions, which are described in a series of papers beginning with Slepian and Pollak,[6] are the eigenfunctions of the finite Fourier transform and give greatly improved resolution and dynamic range from that obtained with conventional ad hoc data windows.

(*ii*) Second, adaptive prewhitening forms a central part of this procedure. This is accomplished by using an autoregressive model of the process, obtained from a pilot estimate of the spectrum, as a *prediction error filter.*

(*iii*) Third, by starting with the pilot spectrum estimate an effective autocorrelation function is realized which is both positive definite and also has low bias. A new technique for generating autoregressive models is described.

(*iv*) Fourth, by replacing the subset averaging used in the Welch technique with a robust combination an improved pilot estimate is frequently obtained.

(*v*) Finally, the *robust filter algorithm* permits accurate estimates of the spectrum to be made when the data contains numerous erroneous data points.

Overall the effect is to give estimates of spectra which are much more reliable than those obtained by conventional methods. The loss calculations reported in Anderson et al.[7] are indicative of its accuracy.

II. THEORETICAL CONSIDERATIONS

In the problems considered here measurements are made of a particular geometric distortion in the waveguide over the length, T, of line.

From these measurements it is desired to estimate the spectrum of the particular distortion. The estimated spectrum is commonly used for two purposes; first to estimate the mode conversion loss, and second, to make inferences on the process used to produce the sample. In both cases frequency resolutions of $1/T$ or better are desirable. But, because the range of the spectra typically encountered in waveguide applications is very large, such resolutions cannot be obtained from simple techniques without obtaining unacceptably biased estimates.

In the literature on spectrum estimation there are numerous papers which are concerned with the trade-off between *resolution* and *variance.* Unfortunately this emphasis on a secondary problem has served to obscure the fundamental conflict between *resolution* and *bias.* The source of this conflict between resolution and bias is a result of fundamental properties of the Fourier transform (see Landau and Pollak).[8] Consider a *direct estimate of spectrum*

$$\hat{S}_D(\omega) = \left| \int_0^T e^{i\omega t} D(t)\, x(t)\, dt \right|^2 \tag{1}$$

in which $D(t)$ is a *data window* or *taper.* If the series, $x(t)$, is a sample of a stationary random process having spectral density function $S(\omega)$ the expected value of such an estimate is given by

$$\mathbf{E}\{\hat{S}_D(\omega)\} = S(\omega) * |\tilde{D}(\omega)|^2 \tag{2}$$

where * indicates convolution and $\tilde{D}$ is the Fourier transform of D. From this formula it can be seen that the expected value of an estimate is the true spectrum convolved with the spectral window, $|\tilde{D}(\omega)|^2$, so that estimates of all nonwhite spectra will be biased.

It is convenient to express this convolution as the sum of a "local" term and a "broad band" component. If the "broad band" component of the bias is defined to be the contribution from frequencies differing from ω by an amount Ω or more by using results from Slepian & Pollak[6] it can be shown that the broad band bias is minimized when D is a *prolate spheroidal wave function.* Further it follows from Slepian[9] that when prolate spheroidal wave functions are used as data windows, the broad band bias can be *bounded* by a quantity which decays asymptotically as $4\sigma^2 T\sqrt{\pi c}\, e^{-2c}$ where $c = \Omega T/2$ so that an immense improvement in performance over conventional windows can be guaranteed for moderate values of c.

Two such windows have been extensively used in the analysis of WT4 data. One of these, used for pilot spectrum estimates and exploratory work, has $c = 4\pi$ and so has a dynamic range of over 100 dB while the second, used in situations where the range of the spectrum is lower and high frequency resolution is required uses $c = \pi$. These data windows

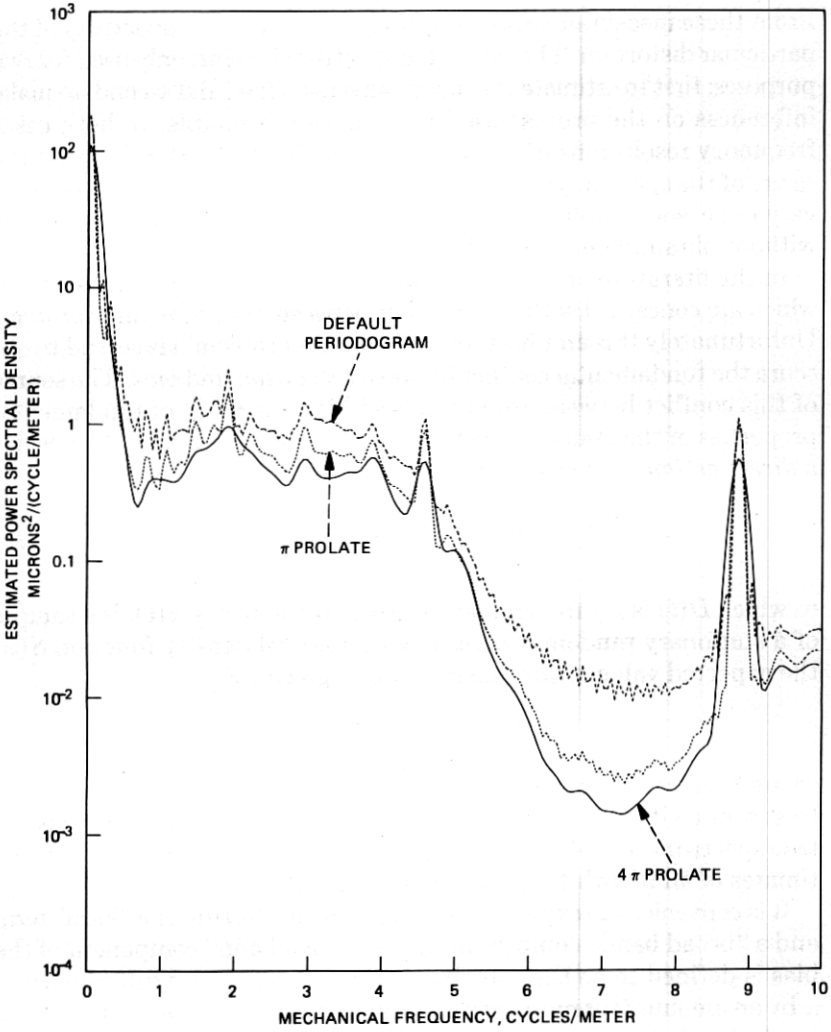

Fig. 1—Comparison of direct spectrum estimates using different data windows. The plotted curves are the average over 2556 data sets.

together with the corresponding spectral windows are shown in Figs. 1 and 2 of Part I.

An example of the different results obtained with different data windows is provided by an analysis of the measured curvature of individual waveguide tubes. The data used here represents the output of a curvature gauge similar to that described in Fox et al.[10] where the curvature is taken from the horizontal sidewall so that the effects of gravitational sag are eliminated and the data are representative of the man-

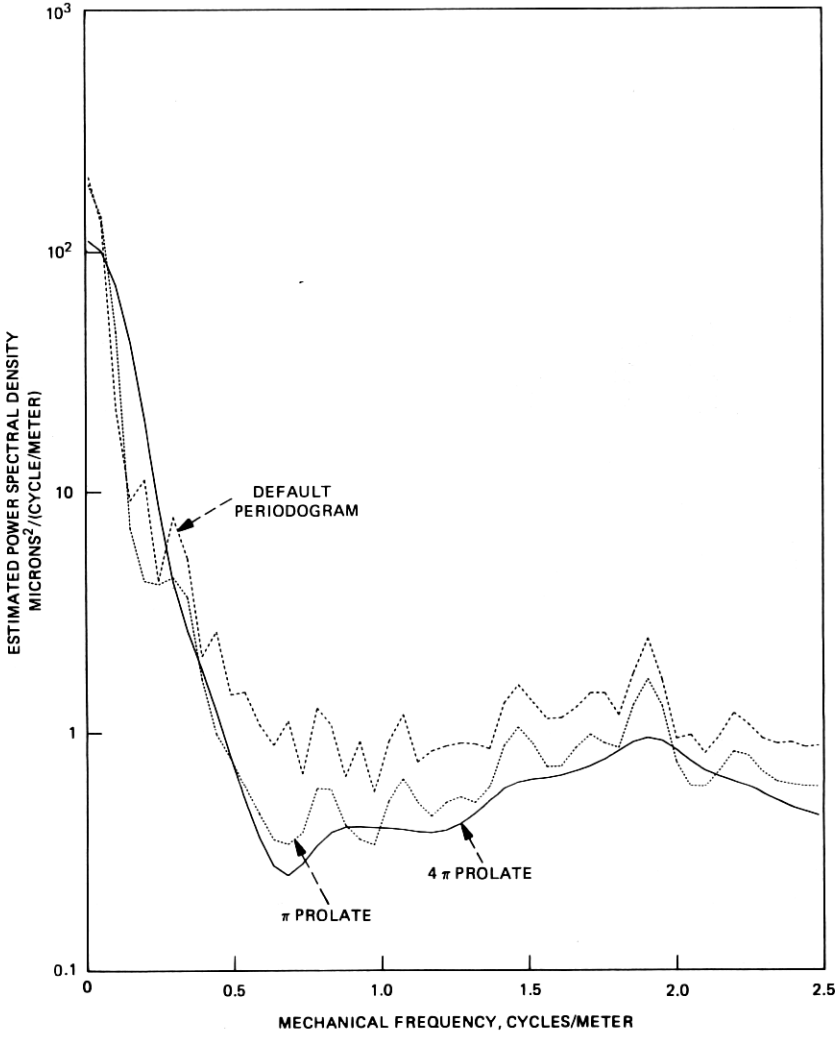

Fig. 2—Low-frequency portion of the data shown in Fig. 1.

ufacturing process. Figure 1 shows the average of 2556 direct estimates of spectra using the two prolate windows described above, and, for comparison, the default periodogram. The differences are most pronounced in the "hole" near 7 cycles per meter but even at low frequencies there are important differences. The region between 0.3 and 1 cycle/meter is particularly important from a mode conversion viewpoint as this region is responsible for the TM_{11} and TE_{12} losses. In this region, shown expanded in Fig. 2, the periodogram is almost a decade higher than the prolate estimates. Also the "structure" evident on the perio-

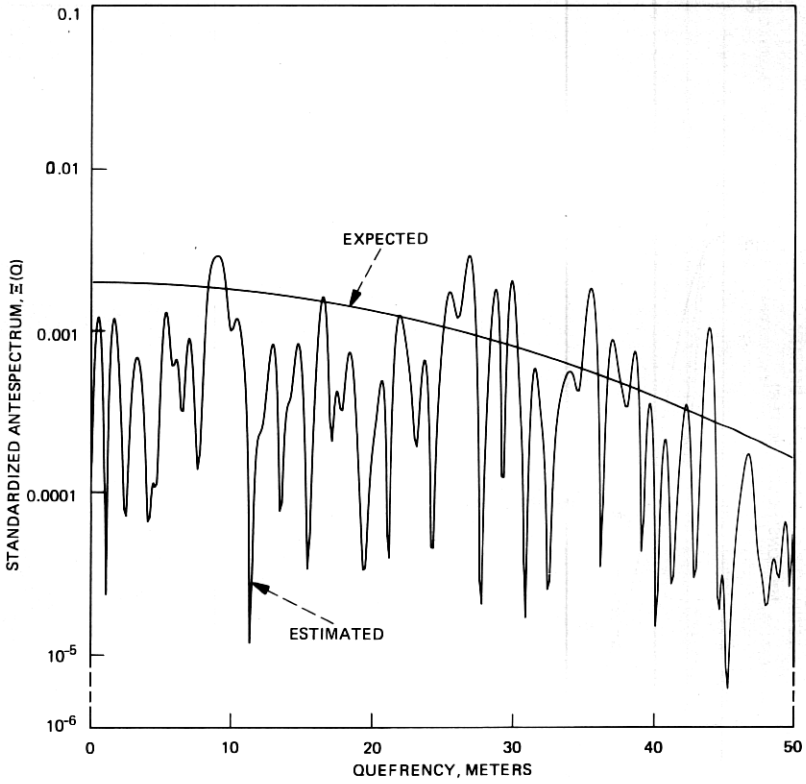

Fig. 3—Expected and standardized sample antespectra for the 19.0 to 20.5 cycle/meter region of the pilot spectrum estimate from mode filter section 17 horizontal curvature.

dogram, for example the peaks at 0.2 and 0.3 cycles per meter, is largely characteristic of it's spectral window (the data sets each contained 808 points spaced 1 cm) rather than the process. It can also be seen that while the π and 4π windows agree in general the narrower window resolves peaks, for example at 0.7 and 1.9 c/m, much better than the broader 4π window but is biased at lower values of the spectrum. In these comparisons it should be noted that since the averages have over 5000 degrees of freedom at each point their standard deviations will be only about 2 percent of their value so that almost all differences between the estimates are significant. Moreover, since the losses are proportional to the spectrum the prolate windows predict losses from the tubes which agrees well with that measured in the field evaluation test whereas those corresponding to the periodogram are considerably larger than the total measured mode conversion loss.

As outlined in Part I a convenient description of the sampling properties of direct estimates is given by the *antespectrum* of the estimate. The antespectrum is the *spectrum of the spectrum estimate* and is ap-

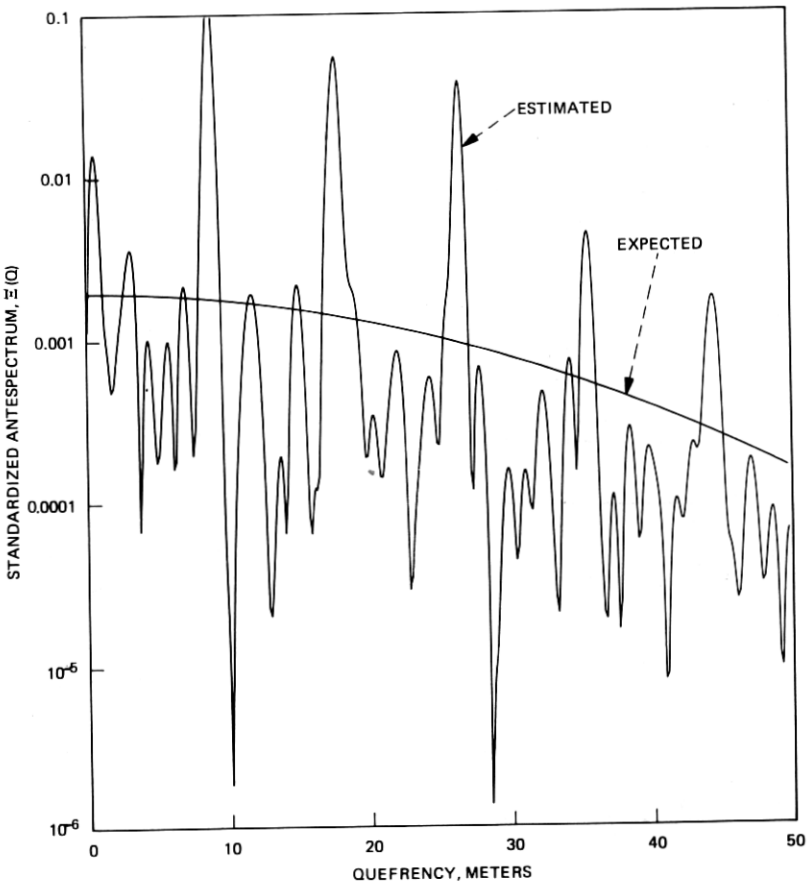

Fig. 4—Antespectra for the 0.5 to 2.0 cycle/meter region.

plicable in regions where the spectrum is constant. In such regions the magnitude of the antespectrum depends on the level of the spectrum and on any smoothing or averaging while its shape depends only on the windows used to generate the spectrum estimate. Since its expected level and shape are known the *sample antespectrum* is a powerful tool for deciding whether a portion of a spectrum is in fact "locally white" or if in fact it contains significant structure. As an example Fig. 3 shows the sample antespectrum corresponding to the 19.0 to 20.5 cycle/meter region† of the pilot spectrum estimate for the horizontal curvature in mode filter section 17 of the field evaluation test (see Anderson et al.[7] for the definition and location of individual mode filter sections such as 17). It

† This region and the one below were chosen as they are both free from obvious peaks and on a plot of the pilot spectrum appear to be flat and very similar.

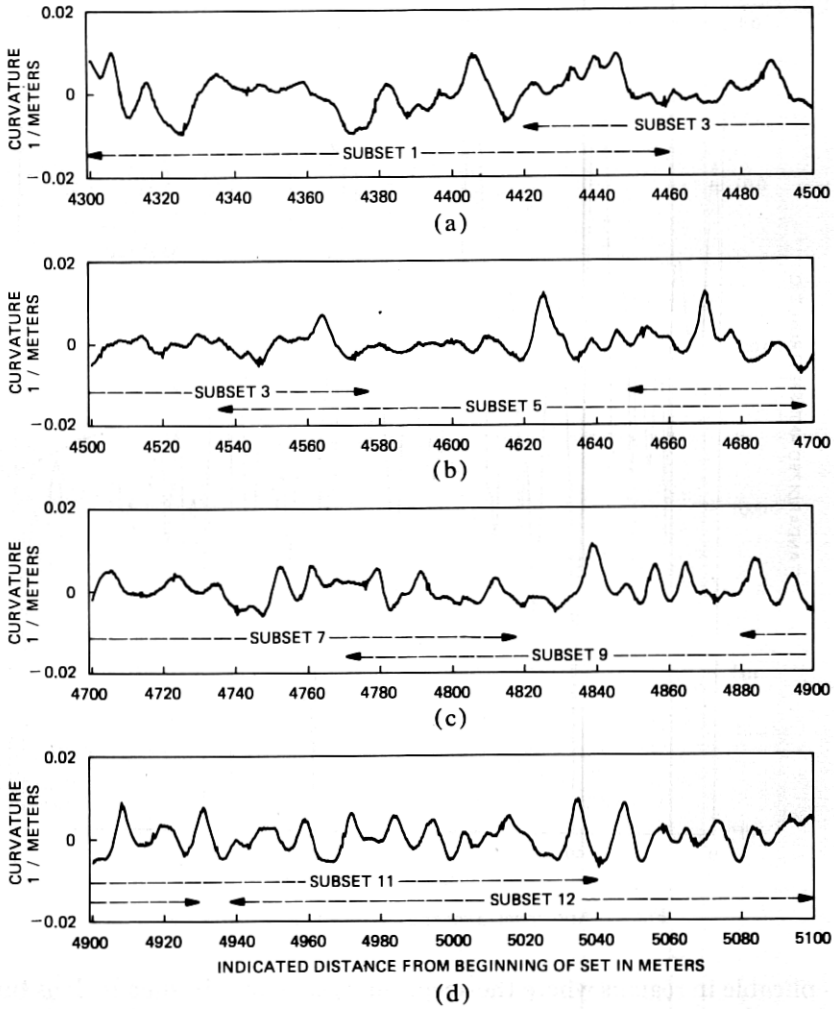

Fig. 5—The vertical curvature for mode filter section 6 as measured by the long-range mouse. Subsets 1, 3, 5, 7, 9, and 11 are used in the test for stationarity; all are used for the pilot estimate.

can be seen that the agreement with the expected behavior is quite good.

In contrast the sample antespectrum shown in Fig. 4, corresponding to the 0.5 to 2.0 cycle/meter region does not conform to the expected shape but rather shows a series of decaying peaks. This shows that a considerable part of the apparent variability of the spectrum in this range is due to the actual fine structure of the spectrum rather than sampling variability. Consequently smoothing must be done very carefully as a smoother with an effective span of only ±8 points will completely obscure

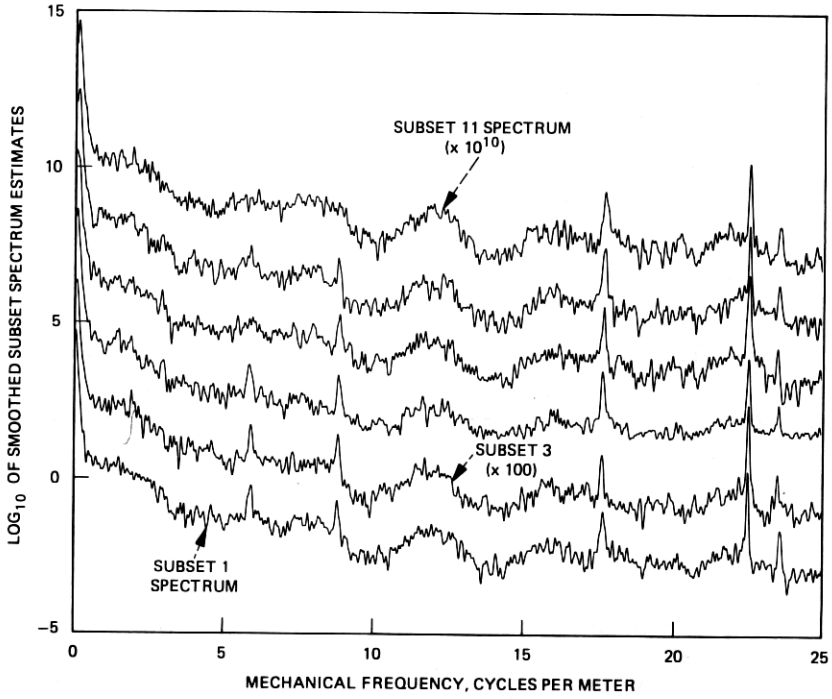

Fig. 6—Smoothed spectrum estimates from alternate subsets of mode filter section 6 vertical curvature. For plotting purposes the estimates have been offset by factors of 100.

this effect. This fine structure in the spectrum is a result of interactions between the tilts and offsets at couplings and, as expected, the random lengths of the individual waveguide tubes is very effective at suppressing the effect at higher frequencies.

III. PILOT SPECTRUM ESTIMATE

The method used to compute the pilot spectrum estimate is a variation of Welch's technique.[5] In this method the data is first divided into several overlapping subsets and a direct estimate of spectrum computed on each subset. For this purpose the prolate data window with $c = 4\pi$ is ideally suited because of its very large dynamic range. For reasons described in Part I the 800-meter mode filter sections were divided into 12 subsets each 160 meters long. These subsets are offset from each other by about 28 to 30 percent of their length so that the information recovery is near optimum. The pilot estimate is a combination of these subset estimates. Originally the combination consisted of a simple arithmetic average over the subsets but in situations where occasional outliers are expected a greatly improved pilot estimate can be obtained by using a simple robust estimate.

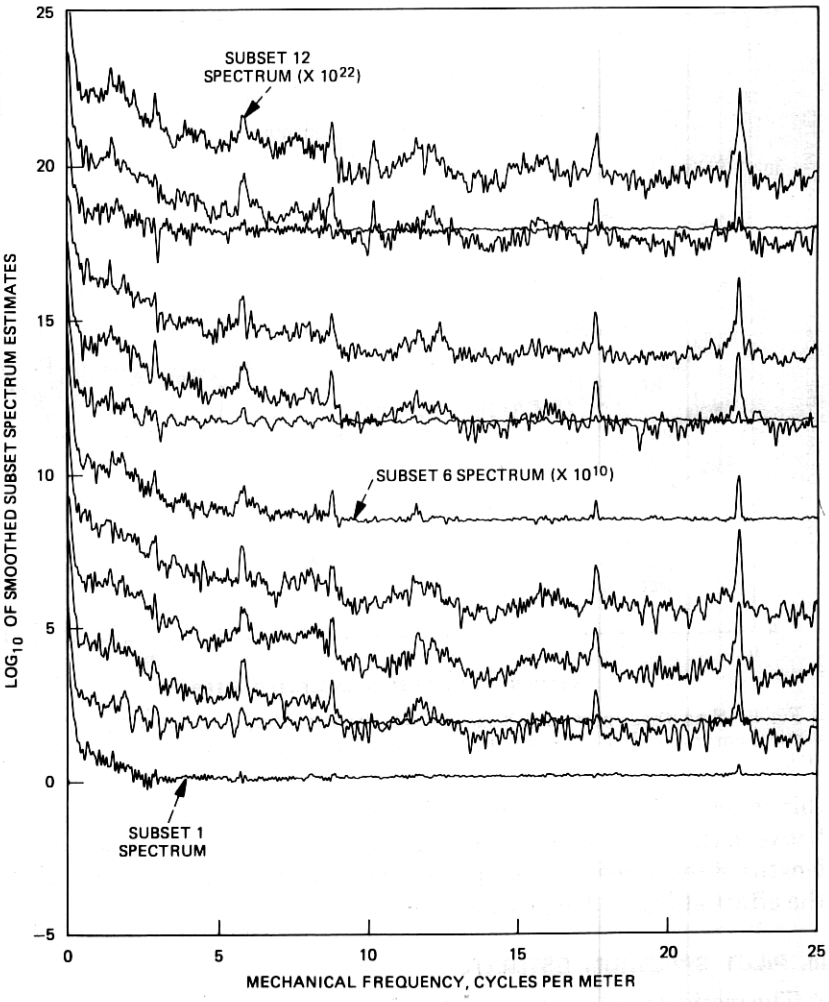

Fig. 7—Smoothed spectrum estimates from all 12 subsets of mode filter section 3 horizontal curvature.

Figure 5 shows a plot of the vertical curvature for mode filter section 6 with the positions of the various subsets indicated. Figure 6 shows alternate subset spectrum estimates and it can be seen that they agree well. So that the plot is readable these estimates have been smoothed and are offset from each other by factors of 100.

By way of contrast, Fig. 7 shows all 12 subset estimates for the horizontal curvature in mode filter section 3 and it can be seen that several of them are "different." The cause of this difference appears to be some small outliers, possibly dust particles. Figure 8 shows the difference between an arithmetic and robust combination of these subsets using

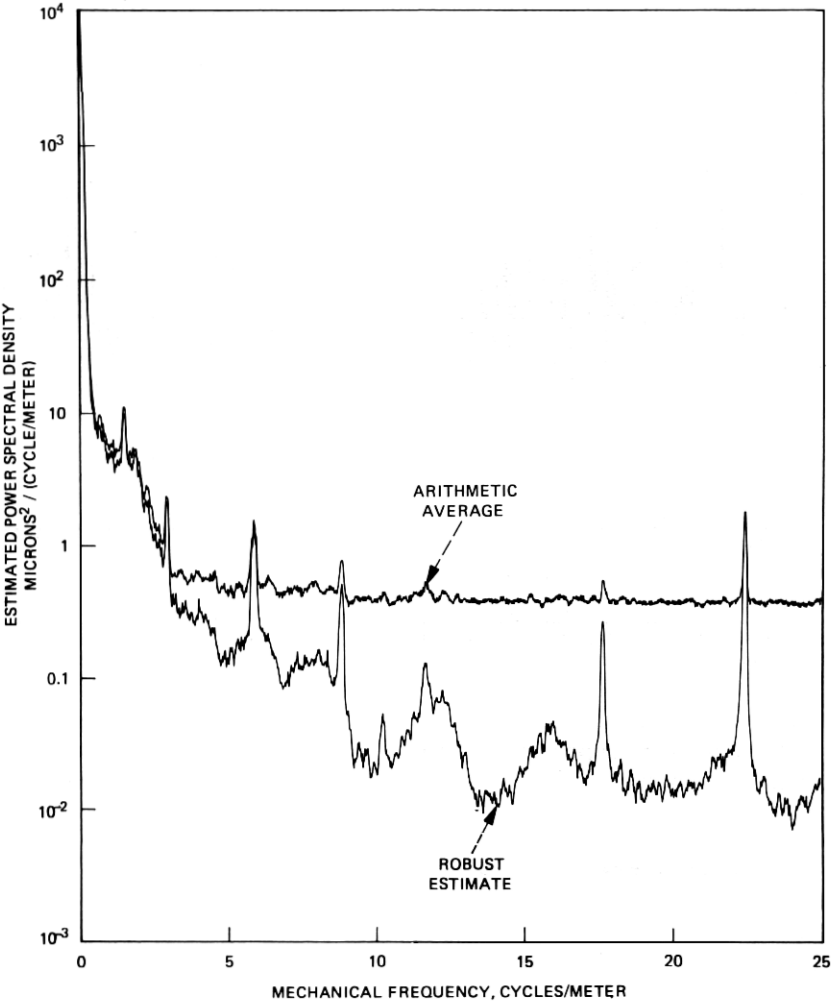

Fig. 8—Comparison of pilot spectrum estimates formed by robust and arithmetic average combinations of the subset spectrum estimates (shown in Fig. 7) for mode filter section 3 horizontal curvature. For plotting purposes both estimates have been smoothed with an adaptive filter having a span of ±10 points.

formula I–5.1 with $k' = 6$. It can be observed that the two differ by more than a decade across much of the frequency band. Integrating the two estimates one finds that the total power decreases by about 10 percent, from 1516 microns^2 for the standard estimate to 1380 microns^2 for the robust estimate. Prediction error, however, is proportional to the integrated logarithm of the spectrum, which decreases dramatically, from 15 microns^2 for the average to 0.101 microns^2 for the robust estimate. Comparisons of these pilot estimates with the spectrum of the individual

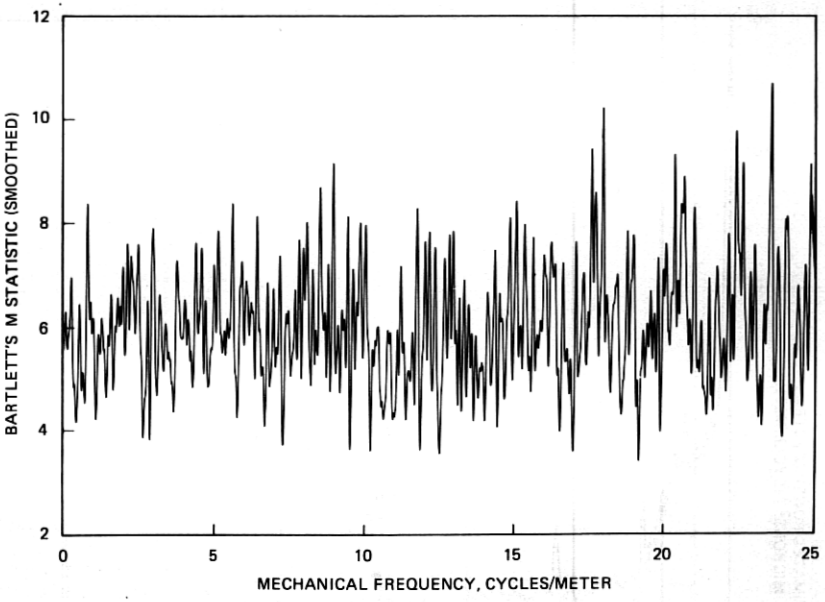

Fig. 9—Comparison of the subset spectrum estimates shown in Fig. 6 for homogeneity using Bartlett's M statistic as a function of frequency. For plotting and interpretative purposes the values shown here have been lightly smoothed.

tubes shown in Fig. 1 indicate that, since the higher frequency portions of the spectrum depend primarily on tubing geometry, the robust estimate is much more believable than the one obtained by simply averaging the subsets.

IV. TESTS FOR STATIONARITY

An important side use of the subset spectrum estimates is in testing the data for stationarity. Tests of this assumption are important in waveguide applications as most models assume that the coupling mechanism between the different modes is driven by a stationary random process and loss estimates made on the basis of such theories will be unreliable of this assumption is violated.

The only test for stationarity which has been found satisfactory is a compound procedure of which the first step is to compute Bartlett's M statistic[11] for heteroscedasticity of variance between subsets as a function of frequency

$$M(\omega) = k\nu \ ln \ \overline{S}(\omega) - \nu \sum_{j=1}^{k} ln \ \overline{S}_j(\omega) \qquad (3)$$

Here $\overline{S}_j(\omega)$ is a slightly smoothed estimate of the spectra of subset j with ν degrees of freedom, and $\overline{S}(\omega)$ is the average, over the k subsets of $\overline{S}_j(\omega)$. If the test is not to be biased constant weight smoothers must be used

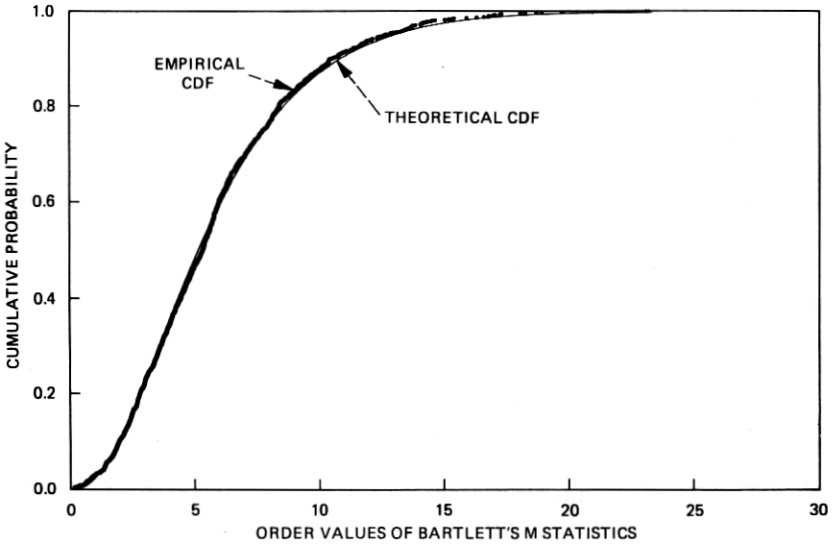

Fig. 10—Comparison of the empirical cumulative distribution function for the *unsmoothed* values of Bartlett's M statistic shown in Fig. 9 with the theoretical distribution. The points used in this test were spaced $4/T$ in frequency. For this comparison the kolmogorov D^- statistic has a value of 0.0264 which is at the 35 percent point.

and smoothing to more than 6 degrees of freedom is inadvisable. Also, so that the test is not biased by correlations between subsets, the subsets used in this test are offset about 57 percent of their length so that, as indicated in Fig. 6, alternate members of the set used to generate the pilot estimate are used in this test.

The second stage of the procedure is to sample $M(\omega)$ at steps greater than $4c/l$, pool the samples, and test for conformance to the known distribution of M. Three primary tests of goodness of fit have been used; the one sided Kolmogorov test D^-, the Anderson-Darling[12] A test, and the Cramer-von Mises W test. (The D and W statistics are described in Durbin.[13]) High values of the Kolmogorov D^+ statistic usually indicate too little variation between the subset spectrum estimates. This condition is normally a result of the subsets being too short.

Figure 9 shows values of M as a function of frequency corresponding to the subset spectrum estimates shown in Fig. 6. The empirical and theoretical distribution functions are plotted in Fig. 10. From this figure it can be seen that the values of M obtained from the different subsets correspond closely to their expected distribution so that the process can be assumed stationary. It should also be noted, see Box,[14] that the M test is very sensitive to departures from the assumed distribution so that, if the spectrum estimates are not closely χ^2 the series will appear nonstationary. Therefore we can conclude that over the frequency band of primary interest, 0 to 25 cycles/meter, the process is stationary and also

that the distribution of losses to a given mode will be χ^2. Other examples are given in Thomson.[15]

V. SMOOTHING

Almost all work on spectrum estimation recommends that various linear smoothers be applied to the raw spectrum estimate and while these procedures are of some value in the present application they can frequently lead to very misleading results. In WT4 applications losses are proportional primarily to the actual value of the spectrum and only to a limited extent to the total power available, and as linear smoothers preserve power rather than spectral amplitudes they cannot be used for loss estimates.

In numerically less critical applications, for example when the spectrum is being "looked at" to study the manufacturing process, conventional smoothing can be seriously misleading and in most applications of this type various adaptive smoothers have been used. While it is impossible to describe the complete details of such smoothers here one of the simpler methods will serve as an example. For this example the bottom curve in Fig. 11 shows a portion of the raw vertical curvature spectrum from mode filter section 14.

(*i*) From a symmetric interval about the frequency of interest values of the raw spectrum estimate are pooled and sorted. From these values a robust estimate of location is made by methods similar to those described in Section 5, Part I, that is, the initial estimate is a systematic function of the order statistics. In this case both ends of the distribution are censored, typically at the 25 percent points, instead of just the upper tail. This initial robust location is shown, offset by a factor of 10, as the second curve of Fig. 11.

(*ii*) The initial robust location estimate is smoothed using a conventional low-pass lifter. The smoothed location estimate is given, offset by a second factor of 10, in the third curve from the bottom.

(*iii*) The central value in the spectrum estimate is compared to the robust local mean. This comparison is made within a window formed by the asymptotic extreme value distribution for distributions of exponential type. Denoting the raw estimate by $\hat{S}(\omega)$ and the smoothed "mean value function" by $\bar{S}(\omega)$ this is accomplished by

$$r = \frac{\hat{S}(\omega)}{\bar{S}(\omega)} \tag{4}$$

so that the window becomes

$$w = \exp\{-v_e e^{-r}\} \tag{5}$$

and the "roughened" estimate is given by

$$S_r(\omega) = w\hat{S}(\omega) + (1 - w)\bar{S}(\omega) \tag{6}$$

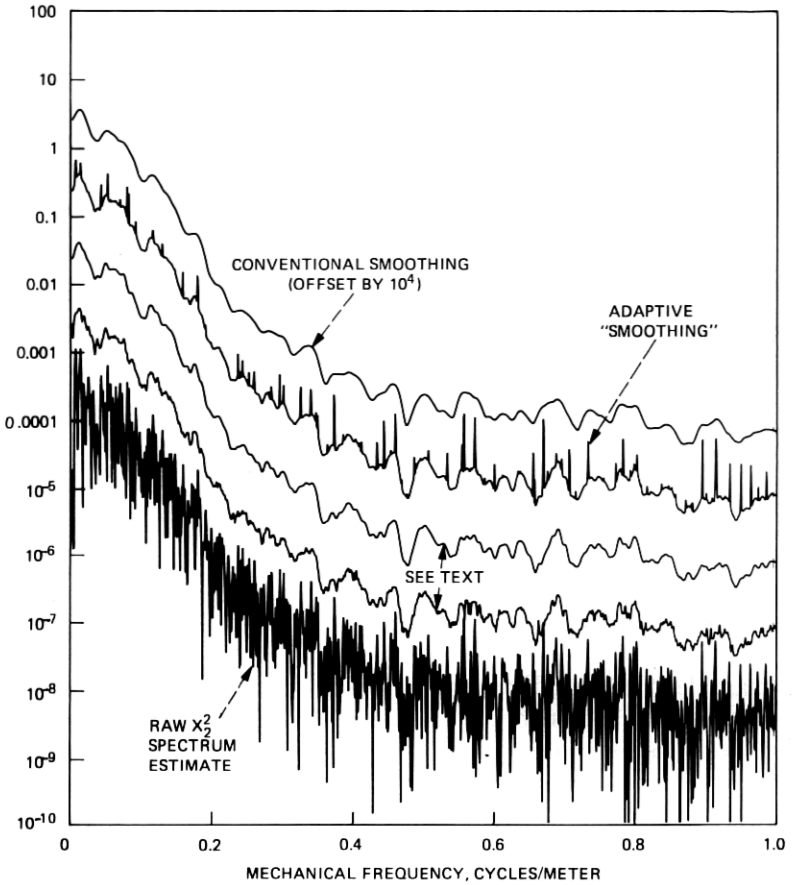

Fig. 11—Steps of a simple adaptive "smoothing" procedure applied to mode filter section 14 vertical curvature spectrum.

This estimate is shown as the fourth curve and the peaks are very evident. For comparison the top curve shows the results of conventional linear smoothing. Comparing the raw, conventional, and robust "smoothed" estimates it is clear that the nonlinear "smoothing" procedure is very helpful in identifying both the basic structure of the spectrum and also any potential periodic components.

VI. ROBUST FILTERING

In addition to the problems already mentioned, conventional estimates of spectra are not *robust,* that is, they are very sensitive to small amounts of erroneous or outlying data. This problem is of particular importance in data of the type obtained in millimeter waveguide problems because of the large range covered by the spectrum and the fact that we are often,

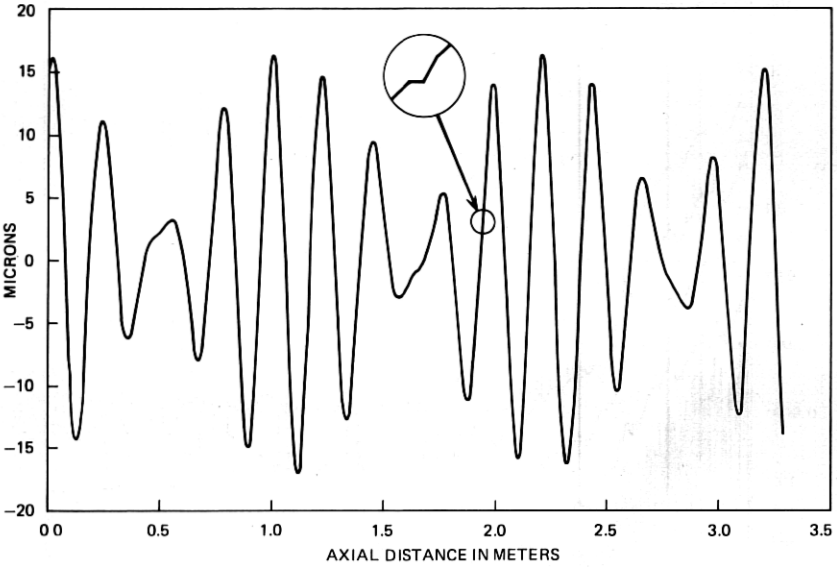

Fig. 12—Plot of the horizontal curvature gauge output for an experimental dielectric-lined waveguide. The insert shows one of two outliers in this data set.

for example in making TM_{11} and TE_{12} loss estimates, interested in the spectral density "at the bottom of a cliff." In this situation there is an aspect to robust estimation which does not appear in the usual situations, namely that an outlier does not have to be "large" to cause serious distortions of the spectral density estimate, but only large with respect to the process innovations variance. In many waveguide spectra, where the innovations variance is less than the process variance by a factor of 10^6 to 10^8 or more, this means that *outliers in time series may not be obvious.* As an example of this phenomena Fig. 12 shows a plot of the horizontal curvature gauge output from an early dielectric lined waveguide in which the outliers are almost invisible under normal plotting conditions but which can be seen when expanded. As will be shown later, such outliers can result in large errors in the estimated spectrum. Further examples are given in Kleiner et al.[16]

The solution which has been found to these problems is known as the *robust filter algorithm.* Basically this procedure uses approximate knowledge of the structure of the process to *predict* the process at the next time step. When the observed value of the process is close to that predicted, the filter simply copies the data. If, on the other hand, the data and prediction differ by a "large" amount, the filter output consists of the prediction. Prediction is used rather than interpolation because the predictor is based on *filtered* values of the process whereas interpolation requires use of data which itself may be contaminated. Also, in the usual

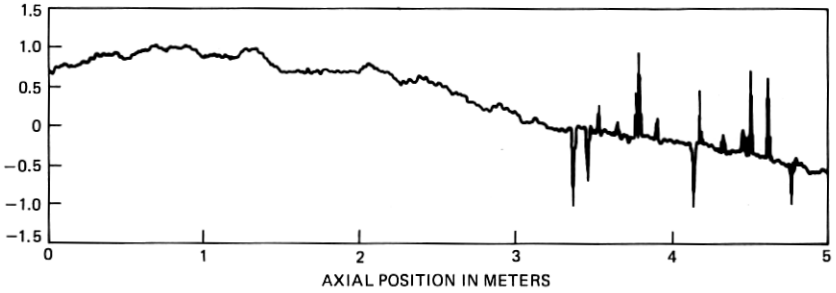

Fig. 13—Simulated waveguide curvature data with outliers. These data were generated using a 54th-order auto regression with a normal innovations sequence.

case where the procedure is combined with prewhitening, the predictive formulation has the important characteristic of having no zeroes in its transfer function on the real frequency axis.

This prediction is made using an autoregressive model of the process. Estimation of the parameters of such a model was described in Part I and further information is available in the recent works of Kailath, Morf, et al.[17,18,19,20]

To a large extent the behavior of the robust filtering algorithm depends on the weight function W and, because of the nonlinearities introduced, improper choice of weight functions can drastically alter the spectrum estimate. To illustrate the behavior of the different influence functions Fig. 13 shows a section of simulated curvature data with a burst of errors between 3 and 5 meters and in Fig. 14 the error sequence

$$\Delta_n = x_n - \hat{x}_n \tag{7}$$

between the original uncontaminated data, x_n and filtered series, $\hat{x}_n$ is shown. In this case the extreme value influence function (Part I, Section 7.7, $u_0 = 4.5$) was used and it can be seen that in the uncontaminated part

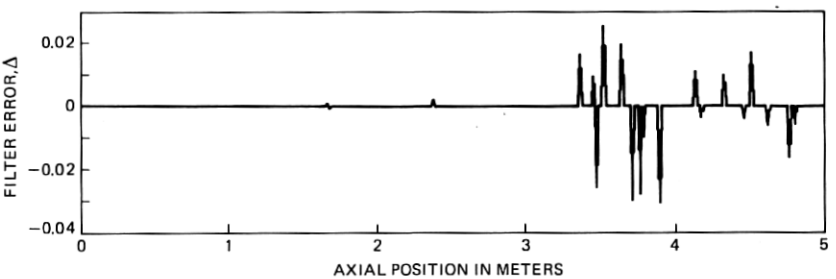

Fig. 14—The error, Δ, between the original uncontaminated data (The contaminated data is shown in Fig. 13) and the sequence obtained by robust filtering using an extreme value influence function with $u_0 = 4.5$. Note the difference in scale between Figs. 13 and 14.

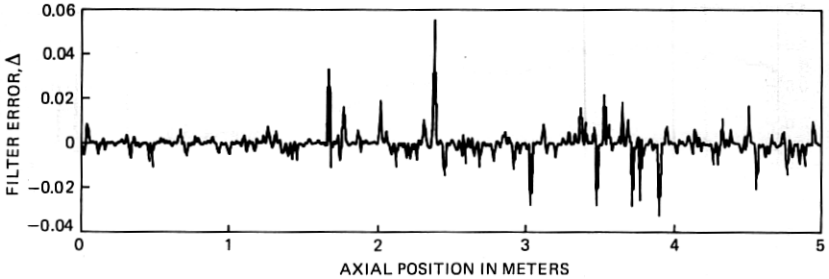

Fig. 15—Filtering error, Δ, between the original uncontaminated data and robust-filtered version using the bisquare influence function with $u_{bs} = 6$. Note the extensive errors occurring in the uncontaminated part of the series.

of the series the error is usually zero or very small. In the contaminated part of the series the errors correspond to the innovations sequence and error propagation is very limited. By contrast Fig. 15 shows the error sequence obtained when the common bisquare influence function

$$\Psi_{bs}(u) = \begin{cases} u[1 - (u/u_{bs})^2]^2 & |u| < u_{bs} \\ 0 & |u| \geq u_{bs} \end{cases} \tag{8}$$

with $u_{bs} = 6$. In this case the error is hardly ever zero, error propagation is general, and in many cases the errors are larger in the uncontaminated data than they are in the contaminated region. In the estimated spectrum these distortions result in spurious peaks and similar errors.

This behavior may be explained by considering the behavior of the filter on uncontaminated autoregressive data of order p so that the error sequence is given by

$$\Delta_n = [I - \Psi]\left(\xi_n + \sum_{k=1}^{p} \alpha_k \Delta_{n-k}\right) \tag{9}$$

where I represents the identity function, Ψ the influence function, and $\{\xi\}$ is the innovations sequence. Because ξ_n is independent of preceding values of Δ_n this equation may be used to compute the probability density function of the errors.

Figure 16 shows the probability density functions for the filter error sequences for three influence functions assuming an autoregressive process of order 1 with $\alpha = 0.9$ and Gaussian innovations. Here, in agreement with the examples shown above (which to simulate waveguide curvature data used an order-54 autoregressive representation), it can be seen that

(*i*) The density corresponding to the extreme value influence function has more than 99 percent of its mass concentrated near the origin and the continuous portion decays rapidly.

(*ii*) The density corresponding to the Huber influence function also

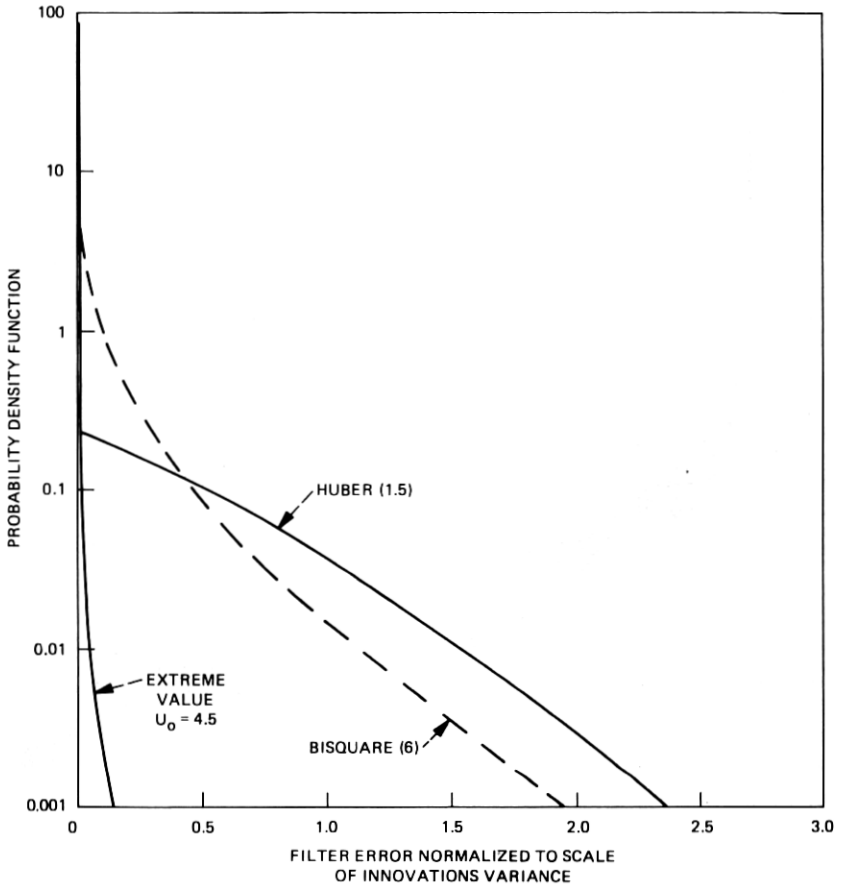

Fig. 16—Probability density functions for the error sequence of a robust filter operating on a first-order autoregressive process with $\alpha = 0.9$. For the extreme value case the density appears to be trimodal with the side modes at ± 6.5 and a level of about 10^{-5}.

has over 75 percent of its mass concentrated at the origin, but away from the origin the density decays more slowly than for the extreme value influence.

(*iii*) For the bisquare influence the density is large and peaked near the origin but is basically continuous and compares with the non-zero error process observed above.

VII. COMPARISON OF SPECTRUM ESTIMATES

Figure 17 shows the average, over 16 mode filter sections, vertical curvature gauge output spectrum from the Netcong WT4 field evaluation trial line computed using the methods described here. These calculations were made separately on each mode filter section and only a single it-

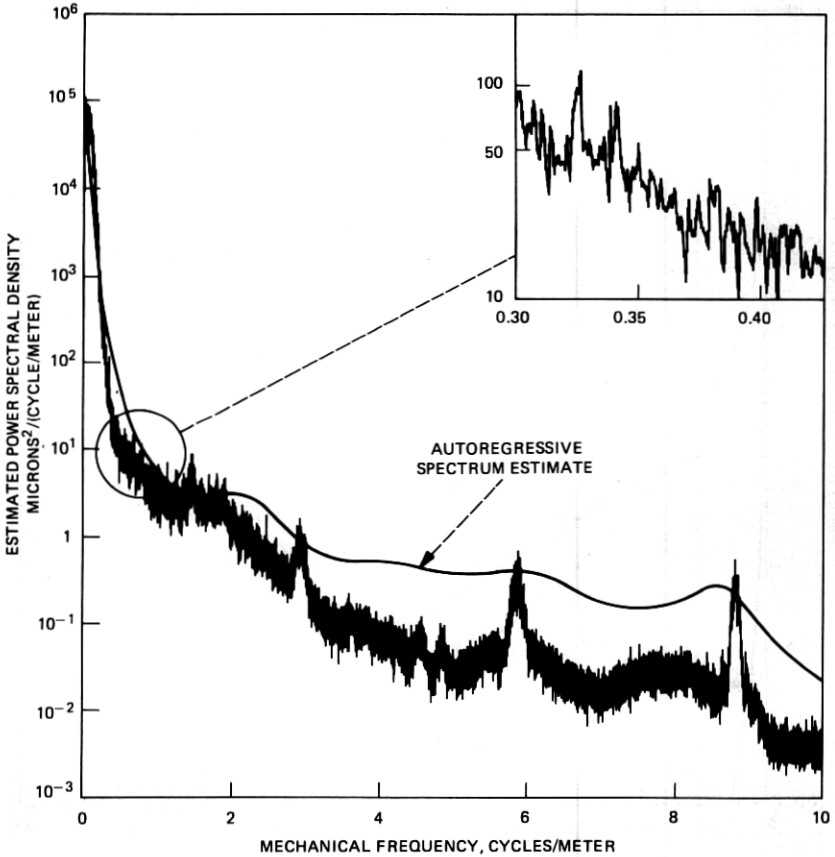

Fig. 17—The average vertical curvature gauge output for mode filter sections 1–10 and 12–17.

eration of the robust filtering procedure was used. The solid line in this plot is an "autoregressive spectrum estimate," the reciprocal of the power transfer function of the prediction error filter normalized by the estimated innovations variance. This particular example was obtained by fitting the averaged pilot estimates with an autoregression of order 54, the median value chosen by Parzen's criterion. It can be seen that the autoregression fits the gross shape of the spectrum fairly well but is completely useless as a description of the fine structure. As a particular example consider the two small peaks near 0.32 cycles per meter (see the expanded portion of the plot). These are completely absent in the autoregressive fit but show clearly in the nonparametric estimate. These peaks, one corresponding to harmonics of the 8.87 meter average tube length and the other to the ~60 foot sheath length were observed in 14 of the 16 mode filter spectra examined and account for considerable

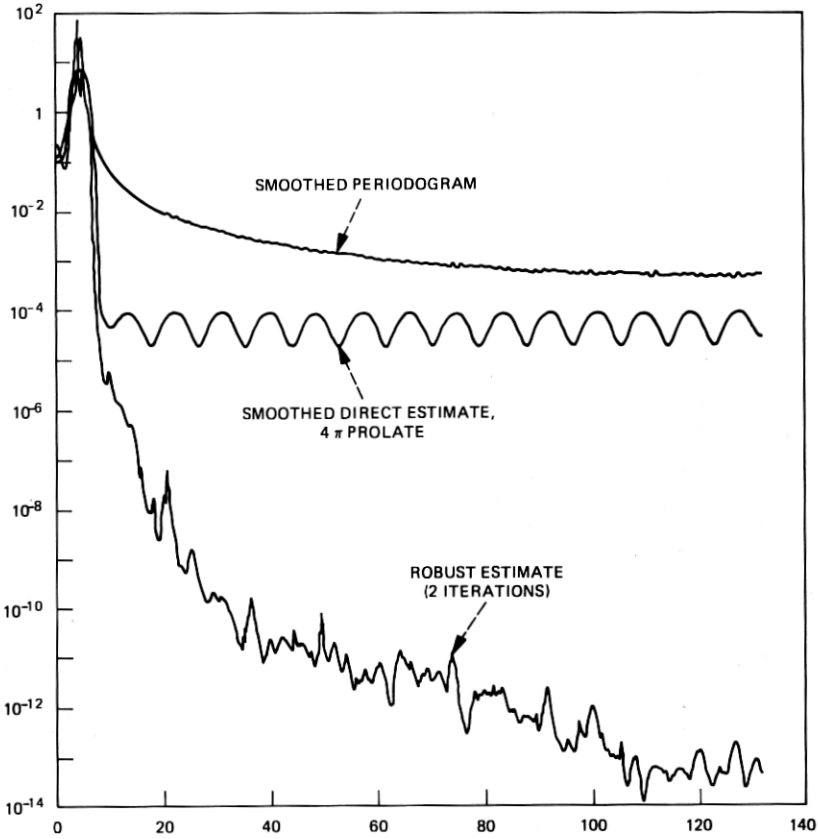

Fig. 18—Comparison of three estimates of spectrum for the data shown in Fig. 12. The systematic oscillations in the center curve are a result of interactions between the two outliers.

TM_{11} mode conversion loss which is confirmed by independent measurements (see Anderson et al.[7]). An even more significant failure of the autoregressive fit to reproduce details is evident at 8.8 cycles per meter. This peak, a result of the straightening operation used in the manufacture of the waveguides, exists in every waveguide tube and is detectable by simple techniques. In this region it can also be noted that, since the autoregressive fit is made to the pilot spectrum estimate, that the robust filtering procedure has improved the noise level by almost a decade and the spectrum estimated for the composite line is comparable with that expected on the basis of the measurements of the individual tubes.

As an example of how effective the robust filter algorithm can be for eliminating the effects of outliers in time series data Fig. 18 shows three different estimates of spectra for the curvature data shown in Fig. 12. The first estimate was computed using the simple extended periodogram;

this result is so badly biased as to be useless over 95 percent of the frequency domain. The second estimate was computed using the 4π prolate taper with the result that, depending on the frequency, the bias of the estimate is reduced by between 1 and 4 decades. While this result is still badly in error the cause of the error is the outliers mentioned earlier rather than limitations of the window. The third estimate uses both the prolate tapers *and* two iterations of the robust filter algorithm and again the estimate changes by *over eight decades* across much of the frequency range. In this estimate one can see details of the spectrum resulting from the manufacturing process rather than from artifacts of the measuring or analysis procedures.

VIII. CONCLUSIONS

Use of the adaptive and robust prewhitening technique in conjunction with data windows defined by prolate spheroidal wave functions has resulted in accurate estimates of spectra where conventional estimates fail. The bias of conventional estimates in situations commonly encountered in the WT4 development is so high that excessive levels of mode conversion are estimated if they are used. The high resolution and low bias properties of these estimates have proven extremely useful in understanding the measured field evaluation test loss data (see Anderson et al.,[7] Carlin and Moorthy[21]). In particular, since the high bias of conventional estimates would have resulted in much higher loss predictions for the TM_{11} and TE_{12} modes (higher in fact than the measured loss) these techniques must be considered a significant factor in the discovery of second-order TM_{21} mode conversion loss.

These procedures also allowed the identification of promising manufacturing techniques and were used extensively to develop, improve and control the manufacturing process. They were incorporated in the continuous monitoring of the waveguide tubing as it was being produced and were a major contributor to the high quality of the present WT4 waveguide.

IX. ACKNOWLEDGMENTS

It is my pleasure to acknowledge the contributions to this work resulting from conversations with B. Kleiner, C. L. Mallows, R. D. Martin, R. L. Pickholtz, D. Slepian, and T. J. West. The data on the individual tubes were supplied by V. J. Tarassov.

REFERENCES

1. D. J. Thomson, "Spectrum Estimation Techniques for Characterization and development of WT4 Waveguide—I," B.S.T.J., *56*, No. 9 (November 1977), pp. 1769–1816.
2. H. Rowe, and W. D. Warters, "Transmission in Multimode Waveguide with Random Imperfections," B.S.T.J., *41*, pp. 1031–1170.

3. J. A. Morrison, and J. McKenna, "Coupled Line Equations with Random Coupling," B.S.T.J., *51,* No. 2 (February 1972), pp. 209–228.
4. L. G. Pusey, *An Innovations Approach to Spectral Estimation and Wave Propagation,* D. S. Thesis, MIT (1975).
5. P. D. Welch, "The Use of the Fast Fourier Transform for Estimation of Spectra: A Method Based on Time Averaging Over Short, Modified Periodograms," IEEE Trans. Audio Electroacoustics, *AU-15* (1967), pp. 70–74.
6. D. Slepian and H. O. Pollak, "Prolate Spheroidal Wave Functions, Fourier Analysis and Uncertainty—I," B.S.T.J., *40,* No. 1 (January 1961), pp. 43–64.
7. J. C. Anderson, et al. "Field Evaluation Test—Transmission Medium Achievements," B.S.T.J., this issue.
8. H. J. Landau, and H. O. Pollak, "Prolate Spheroidal Wave Functions, Fourier Analysis and Uncertainty-II," B.S.T.J., *40,* No. 1 (January 1961), pp. 65–84.
9. D. Slepian, "Some Asymptotic Expansions for Prolate Spheroidal Wave functions," J. Math. Physics, *44,* pp. 99–104.
10. P. E. Fox, S. Harris, and D. J. Thomson, "Mechanical Gauging Techniques," B.S.T.J. this issue.
11. M. S. Bartlett, "Properties of Sufficiency and Statistical Tests," Proc. Roy. Soc., *A 160* (1937), pp. 268–282.
12. T. W. Anderson and D. A. Darling, "Asymptotic Theory of Certain "Goodness of Fit" Criteria Based on Stochastic Processes," Ann. Math. Stat., *23* (1952), pp. 193–212.
13. J. Durbin, *Distribution Theory for Tests Based on the Sample Distribution Function,* SIAM, 1973.
14. G. E. P. Box, "Non-Normality and Tests on Variances," Biometrika, *40* (1953), pp. 318–335.
15. D. J. Thomson, "A Test for Stationarity," in preparation.
16. B. Kleiner, R. D. Martin, and D. J. Thomson, "Robust Estimates of Spectra," in preparation.
17. T. Kailath, Some New Results and Insights in Linear Estimation Theory, Proc. of the IEEE–USSR Joint Workshop on Information Theory, 1975, pp. 97–104.
18. M. Morf, A. Viera, and D. Lee, Ladder Forms for Identification and Speech Processing, Proc. 1977 IEEE Conf. on Decision and Control.
19. M. Morf, A. Viera, D. Lee, and T. Kailath, Recursive Multichannel Maximum Entropy Method, Proc. 1977 Joint Automatic Control Conf., San Francisco, pp. 113–117.
20. M. Morf, D. T. Lee, and A. Viera, Ladder Forms for Detection for Estimation and Detection, presented at the 1977 Intl. Symp. on Information Theory.
21. J. W. Carlin and S. C. Moorthy, "TE_{01} Transmission in Waveguide with Axial Curvature," B.S.T.J., this issue.